AGU PUBLICATIONS

Geophysical Research Letters

RESEARCH LETTER
10.1002/2016GL070923

Key Points:
- Observed factor of 2 in interannual variability (IAV) of ozone dry deposition velocities, dominated by nonstomatal processes
- Stomatal conductance estimates from two observation-driven independent models show similar but weak IAV
- High-quality, long-term measurements needed to identify processes driving IAV in ozone dry deposition

Supporting Information:
- Supporting Information S1

Correspondence to:
O. E. Clifton,
oclifton@ldeo.columbia.edu

Citation:
Clifton, O. E., A. M. Fiore, J. W. Munger, S. Malyshev, L. W. Horowitz, E. Shevliakova, F. Paulot, L. T. Murray, and K. L. Griffin (2017), Interannual variability in ozone removal by a temperate deciduous forest, *Geophys. Res. Lett.*, *44*, 542–552, doi:10.1002/2016GL070923.

Received 19 AUG 2016
Accepted 23 NOV 2016
Accepted article online 5 DEC 2016
Published online 12 JAN 2017
Corrected 6 MAR 2017

This article was corrected on 6 MAR 2017. See the end of the full text for details.

Interannual variability in ozone removal by a temperate deciduous forest

O. E. Clifton[1,2], A. M. Fiore[1,2], J. W. Munger[3], S. Malyshev[4,5], L. W. Horowitz[5], E. Shevliakova[5], F. Paulot[5,6], L. T. Murray[7], and K. L. Griffin[1,2,8]

[1]Department of Earth and Environmental Sciences, Columbia University, New York, New York, USA, [2]Lamont-Doherty Earth Observatory of Columbia University, Palisades, New York, USA, [3]Division of Engineering and Applied Science and Department of Earth and Planetary Sciences, Harvard University, Cambridge, Massachusetts, USA, [4]Cooperative Institute for Climate Science, Princeton University, Princeton, New Jersey, USA, [5]National Oceanic and Atmospheric Administration Geophysical Fluid Dynamics Laboratory, Princeton, New Jersey, USA, [6]Program in Atmospheric and Oceanic Sciences, Princeton, New Jersey, USA, [7]Department of Earth and Environmental Sciences, University of Rochester, Rochester, New York, USA, [8]Department of Ecology, Evolution, and Environmental Biology, Columbia University, New York, New York, USA

Abstract The ozone (O_3) dry depositional sink and its contribution to observed variability in tropospheric O_3 are both poorly understood. Distinguishing O_3 uptake through plant stomata versus other pathways is relevant for quantifying the O_3 influence on carbon and water cycles. We use a decade of O_3, carbon, and energy eddy covariance (EC) fluxes at Harvard Forest to investigate interannual variability (IAV) in O_3 deposition velocities (v_{d,O_3}). In each month, monthly mean v_{d,O_3} for the highest year is twice that for the lowest. Two independent stomatal conductance estimates, based on either water vapor EC or gross primary productivity, vary little from year to year relative to canopy conductance. We conclude that nonstomatal deposition controls the substantial observed IAV in summertime v_{d,O_3} during the 1990s over this deciduous forest. The absence of obvious relationships between meteorology and v_{d,O_3} implies a need for additional long-term, high-quality measurements and further investigation of nonstomatal mechanisms.

1. Introduction

Tropospheric ozone (O_3) is a potent greenhouse gas, deleterious to human health and vegetation, and central to the atmospheric chemistry controlling the removal of air pollutants and reactive greenhouse gases. Attributing observed variability and long-term trends in tropospheric O_3 to specific processes requires a clear understanding of major O_3 sinks [e.g., *Wild*, 2007]. Global atmospheric chemistry models suggest that O_3 dry deposition, the process by which O_3 is taken up by Earth's surface, is 20% of the annual global tropospheric O_3 loss [*Lelieveld and Dentener*, 2000; *Stevenson et al.*, 2006; *Wild*, 2007; *Young et al.*, 2013]. However, O_3 deposition is highly parameterized and varies widely across these models [*Hardacre et al.*, 2015]. Poor mechanistic understanding of the processes leading to O_3 deposition [*Zhang et al.*, 2003; *Pleim and Ran*, 2011; *Wolfe et al.*, 2011] precludes our ability to characterize variability in this sink accurately. Here we examine interannual variability (IAV) in O_3 deposition velocities (v_{d,O_3}) at Harvard Forest, a broadleaf deciduous forest in Massachusetts (MA), USA, using 11 years of O_3 eddy covariance (EC) measurements.

Turbulence above a forest facilitates contact between vegetation and ambient O_3, but the dominant control on daytime v_{d,O_3} is usually the canopy resistance [*Fuentes et al.*, 1992; *Gao and Wesely*, 1995; *Mikkelsen et al.*, 2004], which has stomatal and nonstomatal components [e.g., *Fowler et al.*, 2009]. Stomatal uptake of O_3 is around 40–60% of the total [*Fowler et al.*, 2009] and can be injurious to vegetation [e.g., *Wittig et al.*, 2009; *Ainsworth et al.*, 2012], thereby changing the ability of vegetation to act as an O_3 and carbon sink and transpire water vapor [*Sitch et al.*, 2007; *Sun et al.*, 2012; *Lombardozzi et al.*, 2013]. Variability in nonstomatal deposition is poorly characterized [*Fowler et al.*, 2009; *Rannik et al.*, 2012; *Neirynck et al.*, 2012]. Recent field-based evidence suggests that nonstomatal processes include thermal decomposition and light-mediated and aqueous chemical reactions on vegetation and soil [*Fowler et al.*, 2009; *Ganzeveld et al.*, 2015; *Fumagalli et al.*, 2016]. If deposition is considered to include all of the processes leading to O_3 loss below the top of the canopy, then chemical reactions with biogenic volatile organic compounds (BVOCs) or nitrogen oxide (NO) in canopy air are nonstomatal pathways. However, distinguishing between nonstomatal deposition to surfaces and in-canopy O_3 chemical destruction is relevant for estimating the production of secondary organic aerosol precursors [e.g., *O'Dowd et al.*, 2002; *Hallquist et al.*, 2009].

Several long-term studies show that nonstomatal O_3 deposition dominates the total on a multiyear average basis (e.g., pine plantation [*Fares et al*., 2010], moorland [*Fowler et al*., 2001], spruce forest [*Mikkelsen et al*., 2004], and mixed temperate forest [*Neirynck et al*., 2012]). However, stomatal O_3 deposition dominates the multiyear mean total at a subalpine site [*Turnipseed et al*., 2009] and a boreal forest [*Rannik et al*., 2012]. Although several observational studies demonstrate IAV in flux and some include analysis on IAV in canopy, stomatal, and/or nonstomatal components [*Munger et al*., 1996; *Fowler et al*., 2001; *Mikkelsen et al*., 2004; *Gerosa et al*., 2009; *Fares et al*., 2010; *Rannik et al*., 2012], we lack a complete evaluation of IAV in stomatal versus nonstomatal deposition and the relative contributions to IAV in total deposition.

The present understanding of the controls on variability in v_{d,O_3} over temperate deciduous forests is informed mainly by short-term observational studies [e.g., *Fuentes et al*., 1992; *Finkelstein et al*., 2000]. The decade-long O_3 EC data set from Harvard Forest is unique for temperate deciduous forests. Here we explicitly quantify IAV over 11 years, focusing on v_{d,O_3} in order to probe variability in the strength of this O_3 sink irrespective of near-surface O_3 concentrations. We extend our summertime analysis to stomatal and nonstomatal O_3 deposition and attempt to identify environmental drivers of the v_{d,O_3} IAV. Knowledge of IAV in the depositional sink is necessary to interpret observed long-term trends and IAV in surface O_3.

Current global models typically utilize O_3 dry deposition routines based on the *Wesely* [1989] parameterization ("the Wesely scheme") [e.g., *Hardacre et al*., 2015]. This scheme is designed to represent the diel cycle of deposition on time scales of at least a few weeks and coarse spatial resolution [*Wesely*, 1989]. The Wesely scheme is a resistance-in-series parameterization that includes resistances posed by turbulence, molecular diffusion, and the canopy, which incorporates stomatal and nonstomatal resistances. The rates of nonstomatal deposition in the Wesely scheme do not vary with meteorology aside from solar radiation and canopy wetness.

We show substantial IAV in v_{d,O_3} from O_3 EC measurements at Harvard Forest. This IAV is not simulated by a widely used chemistry-transport model with a modified Wesely scheme. We use the wealth of meteorological and biophysical observations at Harvard Forest to investigate O_3 dry deposition in a traditional resistance-in-series framework, acknowledging limitations with this approach [*Baldocchi et al*., 1987; *Erisman et al*., 1994; *Wesely and Hicks*, 2000]. By using independent methods to determine stomatal conductance and estimating nonstomatal conductance as the residual from the total canopy conductance, we probe the changing roles of stomatal versus nonstomatal O_3 deposition from year to year.

2. Methodology

2.1. Observations at Harvard Forest

Observations are from the red oak-dominated Environmental Measurement Site at Harvard Forest (42°538′N, 72°171′W) in MA, USA [*Munger and Wofsy*, 1999b]. We calculate 11 years (1990–2000) of hourly O_3 deposition velocities (v_{d,O_3}) from O_3 eddy covariance (EC) fluxes and concentrations from 5 m above mean canopy height (24 m) [*Munger et al*., 1996] (Text S1 in the supporting information). Other Harvard Forest micrometeorological and biophysical observations are described in section 2.2, Table S1 in the supporting information, and Texts S2 and S3.

2.2. Resistance-in-Series Framework

O_3 dry deposition is typically described in a resistance-in-series framework analogous to the treatment of resistances in Ohm's law for electrical circuits:

$$v_{d,O_3} = (R_a + R_b + R_c)^{-1} \quad (1)$$

Using the v_{d,O_3} from O_3 EC and other observations at Harvard Forest under this framework, we separate the total resistance (v_{d,O_3}^{-1}) into aerodynamic (R_a), quasi-laminar (R_b), and canopy (R_c) resistances. We focus on stomatal and nonstomatal contributions to canopy conductance ($R_c{}^{-1}$), examining 1 June to 15 September (JJAS15) averages for all quantities as this framework breaks down when the canopy is not fully developed. Averaging across summer also serves to minimize the uncertainty on all components calculated with hourly observations.

The aerodynamic resistance (R_a) is the resistance posed by turbulence and derived from Fick's law. See Text S2 for details on the parameterization used [*Paulson*, 1970; *Businger et al*., 1971; *Högström*, 1988; *Foken*, 2006, 2008; *Meyers et al*., 1998; *Wu et al*., 2015]. The quasi-laminar resistance (R_b) is the resistance posed by molecular diffusion in the boundary layer that forms around individual canopy elements. We adopt the *Wesely and Hicks* [1977] formulation commonly used in the current generation of global models [e.g., *Ganzeveld and Lelieveld*, 1995; *Wang et al*., 1998; *Emmons et al*., 2010] as described in Text S2. Using formulations of R_b that address limitations to the K-theory approach [*Massman*, 1999] or the lack of information about leaf length scales [*Jensen and Hummelshøj*, 1995, 1997] in the formulation used has little influence on our results. We calculate hourly canopy resistance (R_c) using equation (1) and invert to get hourly canopy conductance (g_c). Uncertainties in our g_c estimate result from uncertainties in turbulent flux observations [*Goulden et al*., 1996; *Richardson et al*., 2006] and in the parameterizations of R_a and R_b (Text S2). We remove outliers by requiring hourly g_c to fall within the mean $\pm$ 3 standard deviations of the hourly time series during JJAS15 1992–2000 (i.e., we retain 99.7% of the data; $\mu = 0.51\ \mathrm{cm\ s^{-1}}$ and $\sigma = 0.96\ \mathrm{cm\ s^{-1}}$). We assume that gc is the sum of parallel uptake pathways: stomatal conductance (g_s) and nonstomatal conductance (g_{ns}) [e.g., *Massman et al*., 1994].

$$g_c = g_s + g_{\mathrm{ns}} \tag{2}$$

We calculate hourly g_s using two independent process-level models driven by observations from Harvard Forest. One model incorporates carbon dioxide (CO_2) EC flux, and the other uses water vapor (H_2O) EC flux.

2.3. Stomatal Conductance (g_s) Models

For an estimate of g_s based on H_2O EC, we use the *Shuttleworth et al*. [1984] inversion of the Penman-Monteith equation (hereafter, P-M). We account for the roughly 10% of the observed H_2O flux that comes from below the canopy [*Moore et al*., 1996] by subtracting 10% of hourly H_2O flux before use in P-M, noting that this may be an oversimplification that fails to capture short-term variability. The second g_s estimate, based on CO_2 EC, uses the *Lin et al*. [2015] g_s model (hereafter, L15) based on optimization of photosynthesis and minimization of transpiration [*Cowan and Farquhar*, 1977; *Medlyn et al*., 2011]. We employ gross primary productivity (GPP) at Harvard Forest [*Urbanski et al*., 2007] as the best estimate of net photosynthesis for L15 (GPP may be an upper limit as leaf respiration is not accounted for). We scale both g_s estimates for H_2O by the ratio of O_3 diffusivity to H_2O diffusivity (0.61). See Text S3 for details.

We also use the single-point version of the Geophysical Fluid Dynamics Laboratory (GFDL) land model version 3 (LM3) [*Shevliakova et al*., 2009; *Milly et al*., 2014] configured for Harvard Forest and driven by *Sheffield et al*. [2006] meteorology (combination of reanalysis products and recent observation-based data sets) to examine g_s. LM3 simulates g_s according to *Leuning* [1995] with modification for water stress [*Milly et al*., 2014]. When the simulated leaf area index goes to zero in LM3 due to drought [*Milly et al*., 2014] during August 1991 and 1997 and September 1999, we consider g_s as missing data.

3. Interannual Variability (IAV) in Monthly Mean O_3 Deposition Velocity (v_{d,O_3})

We examine here seasonal cycles of monthly daytime mean v_{d,O_3}. We define daytime as 09:00 A.M. to 03:00 P.M. because there is daylight during this time period for all months of the year. During summer, some years have consistently high (1998 and 1999) or low (1992 and 1996) monthly daytime mean v_{d,O_3} (Figure 1a). In each month, monthly daytime mean v_{d,O_3} during the lowest versus highest year differs by about a factor of 2. Using a bootstrapping technique (Text S4), we find that for each month, the highest and lowest monthly daytime mean v_{d,O_3} are significantly different from each other at a 95% confidence level (Figure 1a). The shapes of the v_{d,O_3} seasonal cycles also differ by year, with the caveat that missing data prevent an illustration of the complete seasonal cycle during several years. Monthly daytime mean O_3 fluxes differ by about a factor of 2 in each month (Figure S1 in the supporting information), but the ranking by year and seasonality of v_{d,O_3} does not simply follow that of the fluxes.

The substantial IAV in v_{d,O_3} from Harvard Forest O_3 eddy covariance (EC) observations is not apparent in 9 years (2004–2012) of daytime mean v_{d,O_3} at Harvard Forest in the Goddard Earth Observing System–Chemistry model (GEOS-Chem) (Figure 1b), a widely used chemistry-transport model with a modified Wesely scheme [*Wang et al*., 1998; *Bey et al*., 2001; *van Donkelaar et al*., 2008] and driven by observed meteorology [*Rienecker et al*., 2011]. While we only have hourly v_{d,O_3} for the years 2004–2012 available from this

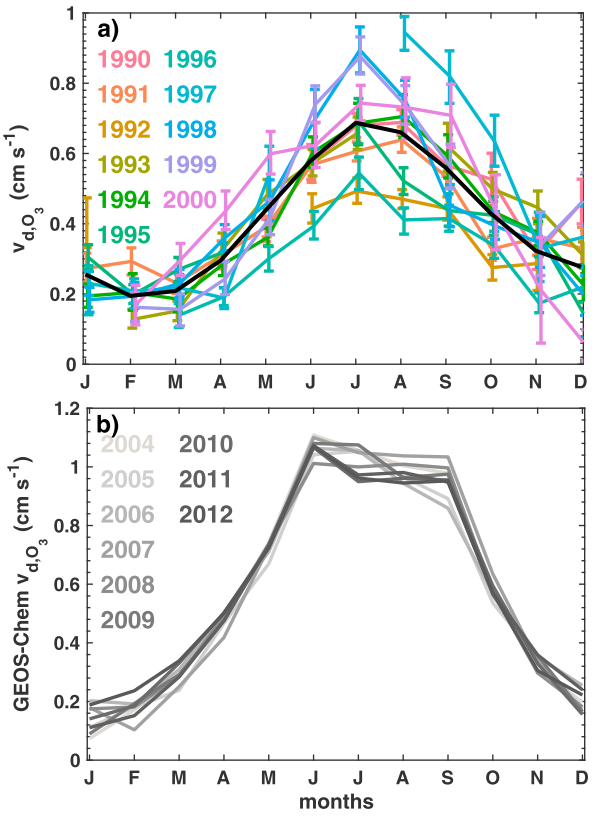

Figure 1. Monthly daytime (09:00 A.M. to 03:00 P.M.) mean O_3 deposition velocity (v_{d,O_3}) at Harvard Forest (a) calculated using a bootstrapping technique (Text S4) on v_{d,O_3} from O_3 eddy covariance observations and (b) from GEOS-Chem (v9-02; http://geos-chem.org; 42°N, 73°W; deciduous land cover type). Black indicates the multiyear mean, and the colors denote the individual years in Figure 1a; the shades of grey denote the individual years in Figure 1b. The error bars in Figure 1a indicate the 95% confidence intervals. If the percentage of days with missing data for any hour between 09:00 A.M. and 03:00 P.M. for a particular month and year is greater than 75%, then the monthly mean is not included.

2° × 2.5° v9-02 simulation, examination of 1990–2000 daily mean v_{d,O_3} from a 4° × 5° v9-01-03 simulation shows a similar lack of IAV. The factors controlling IAV in monthly mean v_{d,O_3} are therefore not represented adequately in GEOS-Chem. As *Walker* [2014] demonstrates a strong sensitivity of surface O_3 over the eastern U.S. to v_{d,O_3} in GEOS-Chem, the poor representation of IAV may lead to model overemphasis of the role of emissions on observed O_3 IAV.

Our understanding of v_{d,O_3} over temperate deciduous forests has been largely based on O_3 EC data sets that span a few years or less: at Kane Experimental Forest from 1997 [*Finkelstein et al.*, 2000; *Finkelstein*, 2001; *Zhang et al.*, 2001, 2002, 2006], Harvard Forest from 1990 to 1994 [*Munger et al.*, 1996] and from 2000 [*Wu et al.*, 2011], and Camp Borden from 1988 [*Fuentes et al.*, 1992; *Padro*, 1996]. The IAV in 11 years of v_{d,O_3} suggests that model development with short-term (weeks to a few years) observations over temperate deciduous forests may restrict model representation to capturing the dynamics of solely high or low v_{d,O_3} years. The lack of IAV in models may contribute to intermodel and model-observation differences that span a factor of 2 in v_{d,O_3} [*Schwede et al.*, 2011; *Park et al.*, 2014; *Val Martin et al.*, 2014; *Hardacre et al.*, 2015]. Understanding the mechanisms responsible for the observed IAV in v_{d,O_3} is crucial to ensure that key processes are incorporated into O_3 deposition parameterizations in the models used to interpret observations and to project changes under emissions and climate scenarios.

The tendency for monthly daytime mean v_{d,O_3} to remain consistent in magnitude during a given summer implies a role for environmental controls that persist over seasonal time scales. We seek to identify climate drivers of this IAV but find no obvious relationship between 1 June and 15 September (JJAS15) mean v_{d,O_3} and net radiation, photosynthetically active radiation, temperature, atmospheric vapor pressure deficit, relative humidity, precipitation [*Boose and Gould*, 1999] , wind speed, wind direction, friction velocity, O_3 concentration or bud break [*Jeong et al.*, 2012] at Harvard Forest, or statewide Palmer Drought Severity Index (Table S1). Soil NO emissions are unlikely to contribute substantially to v_{d,O_3} at Harvard Forest [*Munger et al.*, 1996; *Horii et al.*, 2004].

Recent field-based work [*Mikkelsen et al.*, 2000; *Kurpius and Goldstein*, 2003; *Goldstein et al.*, 2004; *Hogg et al.*, 2007; *Fares et al.*, 2010, 2012, 2014; *Rannik et al.*, 2012; *Neirynck et al.*, 2012; *Launiainen et al.*, 2013] conflicts as to whether in-canopy O_3 destruction by BVOCs such as terpenoids is a key nonstomatal pathway determining variability in observed O_3 deposition. Using June–August mean monoterpene emissions simulated by GEOS-Chem (Table S1), we find that a high v_{d,O_3} year, 1999, matches a high year for monoterpene emission, while 1992 and 1996 are low years for both monoterpene emission and v_{d,O_3}. This finding implies that in-canopy

reactions between terpenoids and O_3 may contribute to IAV in v_{d,O_3}, although the yearly ranking of monoterpene emission magnitude does not simply explain the observed v_{d,O_3} ranking (Table S1).

Figure 1a shows the steep declines in v_{d,O_3} after July during 1995, 1996, 1998, and 1999, all years with late-summertime soil moisture deficits [*Savage and Davidson*, 2001]. For other years, the decline is weaker or shifts to after August–September. The occurrence of drought at Harvard Forest thus may be an important control on the timing of the v_{d,O_3} downturn at the end of summer, with the caveat that soil moisture was not measured during several years.

Half of the full range of JJAS15 daytime mean v_{d,O_3} (0.43 cm s^{-1}) is spanned by years with severe drought (1995 and 1999 [*Savage and Davidson*, 2001]; Table S1). One of these years, 1999, is a high summertime v_{d,O_3} year, whereas daytime mean v_{d,O_3} during the other year, 1995, is 0.01–0.14 cm s^{-1} less than the multiyear mean (Figure 1a). During August–October 1997, a year without a late-summertime drought [*Savage and Davidson*, 2001], the magnitude of v_{d,O_3} is at least 0.11–0.19 cm s^{-1} higher than other years (Figure 1a). Concurrent, longer-term observations of soil moisture and O_3 deposition are needed to pinpoint the role of drought on the ranking of v_{d,O_3} across years at temperate deciduous forests.

Leaf area index (LAI) is a primary driver of seasonality in observed v_{d,O_3} [*Gao and Wesely*, 1995; *Finkelstein et al.*, 2000] and long-term trends in simulated v_{d,O_3} [*Ganzeveld et al.*, 2010; *Wu et al.*, 2012; *Fu and Tai*, 2015], but its role in IAV of v_{d,O_3} is unknown. LAI observations at Harvard Forest from 1998 to 1999 and 2005 to 2014 [*Munger and Wofsy*, 1999a] (Text S2) indicate that LAI during June 1998 is 0.54 and 0.57 m^2 m^{-2} lower than 1999 and the multiyear mean, respectively, due to stunted canopy growth [*Urbanski et al.*, 2007]. June daytime mean v_{d,O_3} during 1998, however, is about the same magnitude as 1999 and 0.14 cm s^{-1} higher than the multiyear mean (Figure 1a), suggesting that the response of v_{d,O_3} to changes in LAI of this magnitude may be weaker than suggested by previous studies [*Charusombat et al.*, 2010; *Schwede et al.*, 2011; *Fu and Tai*, 2015; *Ran et al.*, 2016].

4. Interannual Variability (IAV) in Stomatal Versus Nonstomatal O_3 Deposition

We now examine IAV in 1 June to 15 September (JJAS15) daytime mean O_3 deposition velocities (v_{d,O_3}). We also examine diurnal cycles to probe the mechanisms that control v_{d,O_3}. We find IAV in the shape of the JJAS15 mean diurnal cycle (Figure 2a): some years have a broad daytime maximum (1992 and 1996), while others have a morning or afternoon peak (1993 and 1995 versus 1997 and 2000).

JJAS15 daytime mean canopy resistance (R_c) exceeds both the aerodynamic and quasi-laminar resistances by roughly an order of magnitude (Figure S2), confirming that R_c controls IAV in JJAS15 daytime v_{d,O_3}. We investigate how stomatal and nonstomatal conductances (g_s and g_{ns}) impact IAV in R_c using two process-level g_s models driven by Harvard Forest observations and derived parameters (e.g., GPP; section 2.2 and Text S3). During 1992–2000, JJAS15 daytime mean g_s spans 1.1–1.6 cm s^{-1} for the *Lin et al.* [2015] model (L15) and 0.37–0.54 cm s^{-1} for the *Shuttleworth et al.* [1984] inversion of the Penman-Monteith (P-M) equation. Figure 2b shows the JJAS15 daytime mean g_s for 1992–2000 (values for each year are normalized by the respective multiyear means, which are shown in cm s^{-1} in black asterisks). Despite the discrepancies in magnitude, both estimates consistently show little IAV: the relative interannual spread of daytime mean g_s for 1992–2000 is 10.9% for P-M and 13.8% for L15. Neither approach to estimating g_s yields a ranking of low to high years that matches the v_{d,O_3} ranking (e.g., high g_s years are not high v_{d,O_3} years; Figures 2b and 2c). The similarities in IAV between P-M and L15 suggest that g_s does not control IAV in JJAS15 daytime mean v_{d,O_3} with the caveat that these models may not be sufficiently sensitive to low-frequency environmental controls.

For each g_s estimate, the shape of the mean diurnal cycle for most years deviates little from the shape of the multiyear mean diurnal cycle (Figures 2d, S3b, and S3d). Assuming that existing g_s models can adequately represent IAV in the g_s diurnal cycle, we conclude that deviations from the shape of the climatological v_{d,O_3} diurnal cycle (Figure 2a) are largely controlled by g_{ns}.

We place more confidence in P-M than L15 for the following reasons. First, a recent finding using isotopic methods suggests that standard partitioning between daytime ecosystem respiration and GPP overestimates GPP by 25% during June–July at Harvard Forest [*Wehr et al.*, 2016]. This finding challenges the assumptions inherent in photosynthesis-based approaches to estimate g_s (e.g., L15). Second, the magnitude of P-M g_s is less than g_c (Figure 2d), so P-M g_s can be accommodated in our resistance-in-series framework for O_3 deposition,

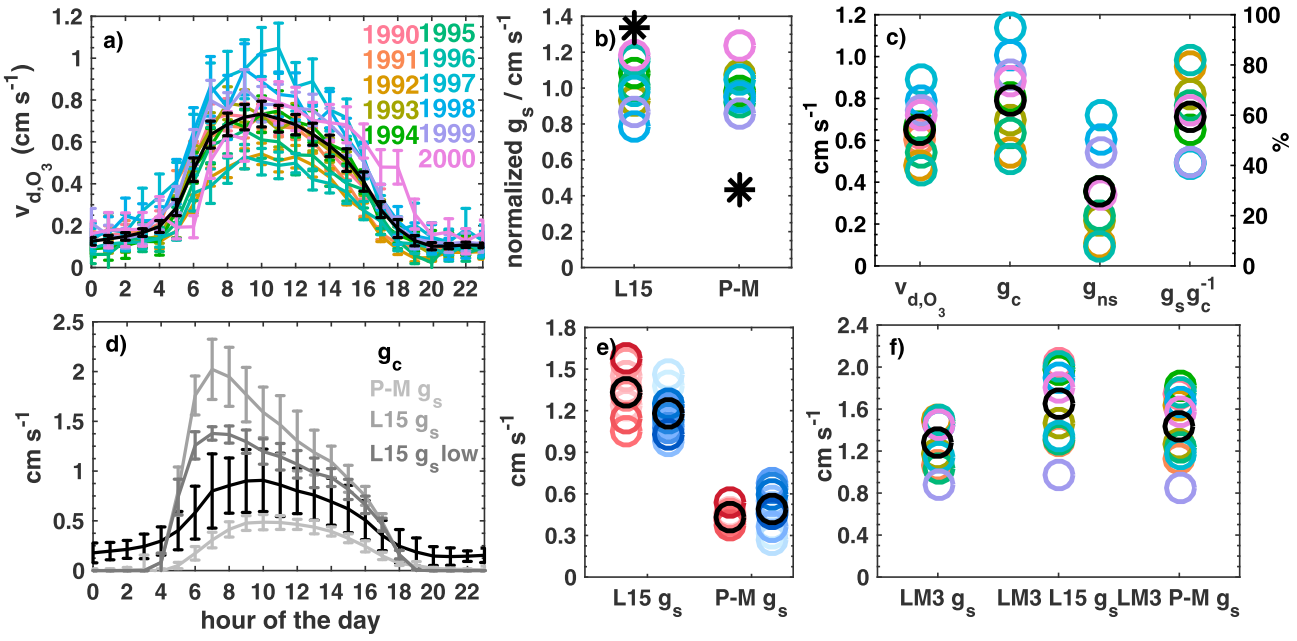

Figure 2. (a) The 1 June to 15 September (JJAS15) hourly mean O_3 deposition velocities (v_{d,O_3}) from observations at Harvard Forest. Black indicates the multiyear mean. The error bars indicate the two standard errors. JJAS15 daytime (09:00 A.M. to 03:00 P.M.) mean (b) L15 and P-M stomatal conductance (g_s) for each year, normalized to the respective multiyear means, which are shown in asterisks in cm s^{-1}, and (c) v_{d,O_3}, canopy conductance (g_c), and nonstomatal conductance (g_{ns}; cm s^{-1}) and the percentage stomatal contribution to g_c ($g_s\ g_c^{-1}$; %); the latter two are inferred using P-M g_s. (d) JJAS15 multiyear hourly mean g_c and g_s from P-M, L15, and L15 without hourly values greater than 3 cm s^{-1} ("L15 g_s low"; cm s^{-1}). The error bars indicate 2 standard deviations (interannual spread). These quantities are calculated using observations during 1992–2000 (section 2.2 and Text S3). (e) JJAS15 daytime mean P-M and L15 g_s (cm s^{-1}) driven by Harvard Forest observations for 1992–2014. The shades of red indicate the years when Harvard Forest O_3 EC observations are available (1992–2000); other years are in shades of blue. Black indicates the multiyear means for 1992–2000 and 2001–2014. (f) JJAS15 daytime mean g_s simulated by GFDL LM3 at Harvard Forest for 1990–2000 and L15 and P-M g_s calculated with LM3-archived fields (Text S5). For all quantities, the seasonal mean by hour has at least 25 days of nonmissing data.

whereas L15 g_s yields an unphysical, negative g_{ns}. We thus use P-M to examine IAV in the relative stomatal contribution to canopy conductance ($g_s\ g_c^{-1}$ or "stomatal fraction") and g_{ns} (Figures 2c, S3c, and S3e).

From year to year, the JJAS15 daytime mean P-M-derived stomatal fraction spans 41–82% (multiyear mean is 59%) at Harvard Forest (Figure 2c). The summertime stomatal fraction over Kane Experimental Forest is 55% for 1997 [*Zhang et al.*, 2006]. Estimates for mixed temperate forests are 34% for 2002 [*Hogg et al.*, 2007], 28% for 2000–2010 [*Neirynck et al.*, 2012], 50% for 1998 [*Zhang et al.*, 2006], and 47% for 2007 [*Nunn et al.*, 2010]. JJAS15 mean g_s accounts for a substantial fraction of g_c each year at Harvard Forest, but the variance in P-M g_s across years is 5% of the variance in daytime mean g_c, in contrast to 106% for P-M-derived g_{ns}. The ranking across years of v_{d,O_3} and g_c is similar to that of g_{ns} (and the inverse that of the stomatal fraction; Figure 2c), implying that g_{ns} drives IAV in v_{d,O_3}.

Meteorological and carbon and energy eddy covariance (EC) measurements have continued after O_3 EC was discontinued at Harvard Forest, allowing us to compute P-M and L15 for more recent years (Figures 2e and S4). The relative interannual spreads in P-M and L15 g_s estimates are 26.9% and 11.6% for 2001–2014. While the relative spread in L15 slightly decreases, the P-M relative spread for 2001–2014 is 2.5 times that for 1992–2000. This finding raises the possibility of decadal variability in the contribution of g_s to IAV in g_c. Our conclusion that g_{ns} drives IAV in JJAS15 mean v_{d,O_3} thus may be limited to 1992–2000. O_3 deposition and coincident meteorological observations are needed for several decades to elucidate more clearly the impact of IAV in g_s on g_c.

We return to 1990–2000 to examine g_s as simulated by GFDL LM3 at Harvard Forest. The relative interannual spread of JJAS15 daytime mean LM3-simulated g_s is 18.3%, slightly higher but similar to that for the 1990–2000 observation-driven estimates. The ranking of years for LM3-simulated g_s does not follow that for v_{d,O_3} from O_3 EC (Figures 2c and 2f), consistent with our conclusion from the observation-driven g_s estimates that IAV in g_s does not control IAV in v_{d,O_3} at Harvard Forest during the 1990s. Similar to the

observation-driven L15 g_s, we find that the LM3-simulated g_s is greater than g_c, indicating unphysical, negative g_{ns} (Figures 2c and 2f). Even if we scale the LM3-simulated g_s to the magnitude of the observation-driven P-M 1992–2000 JJAS15 daytime mean g_s (Figure 2b), the variance only explains 14% of the variance in g_c across years, implying a dominant role for IAV in g_{ns} on g_c.

We use LM3 to test how well the P-M and L15 approaches capture the IAV in LM3-simulated g_s (Figures 2f and S5). P-M and L15 g_s are calculated from archived fields (Text S5). Relative interannual spreads are similar but slightly higher for LM3-driven L15 and P-M estimates (22.5% and 21.9%) than for LM3-simulated g_s. The LM3-driven P-M and L15 approaches emulate the ranking across years in LM3-simulated g_s (Figure 2f), indicating that both methods are capable of capturing IAV in LM3-simulated g_s. This consistency across independent approaches lends confidence to constraining g_s IAV using observation-driven P-M and L15.

The diurnal course of summertime mean g_s remains uncertain. The 1992–2000 multiyear mean diurnal cycle calculated via P-M has a broad daytime maximum, whereas L15 simulates g_s with an early-morning peak declining into the afternoon (Figures 2d, S3b, and S3d). This early-morning peak in observation-driven L15 g_s also occurs in LM3-driven L15 (Figure S5) but is produced neither by LM3 (Figure S5) nor by P-M estimates (Figures 2d, S5, and S3b). Leaf-level g_s measurements during summers 1991–1992 [*Bassow and Bazzaz*, 1999] offer little constraint on the summertime mean diurnal cycle (Figure S6). Differences (IAV, magnitude, diurnal-cycle shape) between observation-driven L15 and P-M for 1992–2000 lessen when we omit hourly g_s greater than 3 cm s^{-1} from L15 (Figure 2d). For 84% of times that g_s is greater than 3 cm s^{-1} during JJAS15 for 05:00 A.M. to 06:00 P.M., atmospheric vapor pressure deficit (VPD) is less than 0.02 kPa, suggesting that some of the differences between P-M and L15 are from the sensitivity of g_s to low VPD in L15. Note that when L15 g_s is greater than 3 cm s^{-1} during JJAS15 05:00 A.M. to 06:00 P.M., mean GPP is 1.3 mol m^{-2} s^{-1} lower when VPD is less than 0.02 kPa. If stomatal and nonstomatal processes operate most strongly at different times of the day, constraining the stomatal contribution to the summertime mean diurnal cycle of v_{d,O_3} should provide insight into driving nonstomatal mechanisms.

5. Discussion and Conclusion

The understanding of O_3 removal by temperate deciduous forests, prevalent over the eastern USA, is largely based on short-term observations, with interannual variability (IAV) in O_3 deposition receiving little attention. However, source attribution and top-down approaches using observations (e.g., satellite data) to infer precursor emissions and their IAV rely on accurate estimates of sinks such as O_3 dry deposition. Our analysis using 11 years (1990–2000) of O_3 eddy covariance (EC) at Harvard Forest, a broadleaf deciduous forest in the northeastern USA, reveals substantial IAV in O_3 deposition velocities (v_{d,O_3}). This IAV is not captured by a chemistry-transport model with a modified *Wesely* [1989] dry deposition scheme that is frequently applied for source attribution, despite a known model sensitivity of surface O_3 over the eastern USA to O_3 deposition [*Walker*, 2014].

Examining O_3 dry deposition in the traditional resistance-in-series framework with two independent stomatal conductance (g_s) models driven by Harvard Forest observations, we conclude that IAV in summertime v_{d,O_3} during 1992–2000 mainly reflects nonstomatal processes. During other periods (e.g., 2001–2014), stomatal uptake may contribute substantially to IAV in v_{d,O_3} at Harvard Forest, as suggested by a factor of 2 increase in IAV in g_s estimated from H_2O EC during 2001–2014 (when O_3 EC are unavailable) versus 1992–2000. Constraining stomatal O_3 uptake is necessary to quantify the impacts of O_3-induced damage on long-term trends and variability in GPP [e.g., *Sitch et al*., 2007; *Fares et al*., 2013; *Yue et al*., 2016] and water use efficiency [e.g., *Keenan et al*., 2013, 2014; *Holmes*, 2014; *Hoshika et al*., 2015; *Lombardozzi et al*., 2015].

Summertime daytime mean nonstomatal conductance as inferred from the g_s estimate based on H_2O EC at Harvard Forest varies from 20 to 58% of canopy conductance during 1992–2000 (41% on a multiyear basis). Similarly, the range of the summertime daytime mean nonstomatal contribution is 43–65% during 2001–2006 (multiyear mean is 52%) at a ponderosa pine plantation [*Fares et al*., 2010]. The nonstomatal contribution to total deposition during a growing season or on a multiyear basis is also substantial (greater than 25%) at other temperate deciduous and mixed forests [*Zhang et al*., 2006; *Hogg et al*., 2007; *Nunn et al*., 2010; *Neirynck et al*., 2012] and over other land cover types [*Zeller and Nikolov*, 2000; *Fowler*

et al., 2001; *Mikkelsen et al*., 2004; *Altimir et al*., 2006; *Cieslik*, 2009; *Gerosa et al*., 2009; *Rannik et al*., 2012; *Fares et al*., 2012, 2014; *Zona et al*., 2014].

Pinpointing the role of climatic drivers of IAV in O_3 dry deposition will improve projected changes of this process with climate. The persistent IAV in the magnitude of monthly mean v_{d,O_3} at Harvard Forest during summer 1990–2000 suggests that longer-term (several weeks to months) environmental conditions determine the magnitude of nonstomatal conductance and subsequently low versus high v_{d,O_3} years. Earlier studies [*Bauer et al*., 2000; *Gerosa et al*., 2009; *Rannik et al*., 2012] also suggest that there are longer-term controls on O_3 dry deposition. We find that the environmental variables (e.g., relative humidity, friction velocity, temperature, solar radiation, and NO concentration [*Fowler et al*., 2001; *Zhang et al*., 2002; *Altimir et al*., 2006; *Hogg et al*., 2007; *Lamaud et al*., 2009; *Coyle et al*., 2009; *Rannik et al*., 2012; *Neirynck et al*., 2012]) shown to influence daytime nonstomatal deposition on various time scales during summer at other monitoring sites do not emerge as controls on summertime mean IAV at Harvard Forest. However, the generalizability of O_3 deposition observations at Harvard Forest and other sites needs to be established. Combining long-term ecosystem-scale measurements over different land cover types is necessary for reliable scaling for global O_3 dry deposition estimates.

In-canopy O_3 destruction by terpenoids may contribute to nonstomatal deposition at Harvard Forest even though the forest is not considered to emit high terpene levels [*McKinney et al*., 2011]. We speculate that IAV in v_{d,O_3} at Harvard Forest is controlled by multiple nonstomatal depositional pathways, such as thermal decomposition and aqueous reactions on water films and light-mediated reactions on leaf waxes and soil and in-canopy chemistry [*Fowler et al*., 2009; *Fumagalli et al*., 2016], that vary in complex ways with environmental parameters. We emphasize the need for multidecadal observations over temperate deciduous forests to quantify nonstomatal versus stomatal O_3 deposition and attribute variability to meteorological and biophysical drivers.

Acknowledgments

We acknowledge support from NOAA grant NA14OAR4310133 and an NSF Graduate Research Fellowship (DGE-16-44869) to O.E.C. Harvard Forest observations were supported in part by the U.S. Department of Energy, Office of Science (BER), and NSF Long-Term Ecological Research. O.E.C. acknowledges a useful conversation with Harald Rieder. Please contact O.E.C. for the data used here. This is Lamont-Doherty Earth Observatory contribution 8077. We acknowledge the useful comments and feedback from two anonymous reviewers.

References

Ainsworth, E. A., C. R. Yendrek, S. Sitch, W. J. Collins, and L. D. Emberson (2012), The effects of tropospheric ozone on net primary productivity and implications for climate change, *Annu. Rev. Plant Physiol. Plant Mol. Biol*, doi:10.1146/annurev-arplant-042110-103829.

Altimir, N., P. Kolari, J.-P. Tuovinen, T. Vesala, J. Bäck, T. Suni, M. Kulmala, and P. Hari (2006), Foliage surface ozone deposition: A role for surface moisture?, *Biogeosciences*, *3*, 209–228.

Baldocchi, D. D., B. B. Hicks, and P. Camara (1987), A canopy stomatal resistance model for gaseous deposition to vegetated surfaces, *Atmos. Environ.*, *21*(1), 91–101.

Bassow, S., and F. Bazzaz (1999), Canopy photosynthesis study at Harvard Forest 1991–1992, HF059, Harvard Forest Data Archive, Harvard Forest, Petersham, Mass.

Bauer, M. R., N. E. Hultman, J. A. Panek, and A. H. Goldstein (2000), Ozone deposition to a ponderosa pine plantation in the Sierra Nevada Mountains (CA): A comparison of two different climatic years, *J. Geophys. Res.*, *105*, 22,123–22,136, doi:10.1029/2000JD900168.

Bey, I., D. J. Jacob, R. M. Yantosca, J. A. Logan, B. D. Field, A. M. Fiore, Q. Li, H. Y. Liu, L. J. Mickley, and M. G. Schultz (2001), Global modeling of tropospheric chemistry with assimilated meteorology: Model description and evaluation, *J. Geophys. Res.*, *106*, 23,073–23,095, doi:10.1029/2001JD000807.

Boose, E., and E. Gould (1999), *Shaler Meteorological Station at Harvard Forest 1964–2002, HF000*, Harvard Forest Data Archive, Harvard Forest, Petersham, Mass.

Businger, J. A., J. C. Wyngaard, Y. Izumi, and E. F. Bradley (1971), Flux-profile relationships in the atmospheric surface layer, *J. Atmos. Sci.*, *28*, 181–189.

Charusombat, U., D. Niyogi, A. Kumar, X. Wang, F. Chen, A. Guenther, A. Turnipseed, and K. Alapaty (2010), Evaluating a new deposition velocity module in the Noah land-surface model, *Boundary-Layer Meterol.*, *137*, 271–290, doi:10.1007/s10546-010-9531-y.

Cieslik, S. (2009), Ozone fluxes over various plant ecosystems in Italy, *Environ. Pollution*, *157*, 1487–1496, doi:10.1016/j.envpol.2008.09.050.

Cowan, I. R., and G. D. Farquhar (1977), Stomatal function in relation to leaf metabolism and environment, in *Integration of Activity in the Higher Plant*, edited by D. H. Jennings, pp. 471–505, Cambridge Univ. Press, Cambridge, U. K.

Coyle, M., E. Nemitz, R. Storeton-West, D. Fowler, and J. N. Cape (2009), Measurements of ozone deposition to a potato canopy, *Agric. For. Meteorol.*, *149*, 655–666, doi:10.1016/j.agrformet.2008.10.020.

Emmons, L. K., et al. (2010), Description and evaluation of the Model for Ozone and Related chemical Tracers, version 4 (MOZART-4), *Geosci. Model Dev.*, *3*, 43–67, doi:10.5194/gmd-3-43-2010.

Erisman, J. W., A. Van Pul, and P. Wyers (1994), Parameterization of surface resistance for the quantification of atmospheric deposition of acidifying pollutants and ozone, *Atmos. Environ.*, *28*(16), 2595–2607, doi:10.1016/1352-2310(94)90433-2.

Fares, S., M. McKay, R. Holzinger, and A. H. Goldstein (2010), Ozone fluxes in a *Pinus ponderosa* ecosystem are dominated by non-stomatal processes: Evidence from long-term continuous measurements, *Agric. For. Meteorol.*, *150*(3), 420–431, doi:10.1016/j.agrformet.2010.01.007.

Fares, S., R. Weber, J. H. Park, D. Gentner, J. Karlik, and A. H. Goldstein (2012), Ozone deposition to an orange orchard: Partitioning between stomatal and non-stomatal sinks, *Environ. Pollut.*, *169*, 258–266, doi:10.1016/j.envpol.2012.01.030.

Fares, S., R. Vargas, M. Detto, A. H. Goldstein, J. Karlik, E. Paoletti, and M. Vitale (2013), Tropospheric ozone reduces carbon assimilation in trees: Estimates from analysis of continuous flux measurements, *Global Change Biol.*, *19*, 2427–2443, doi:10.1111/gcb.12222.

Fares, S., F. Savi, J. Muller, G. Matteucci, and E. Paoletti (2014), Simultaneous measurements of above and below canopy ozone fluxes help partitioning ozone deposition between its various sinks in a Mediterranean oak forest, *Agric. For. Meteorol.*, *198*, 181–191, doi:10.1016/j.agrformet.2014.08.014.

Finkelstein, P. L., T. G. Ellestad, J. F. Clarke, T. P. Meyers, D. B. Schwede, E. O. Hebert, and J. A. Neal (2000), Ozone and sulfur dioxide dry deposition to forests: Observations and model evaluation, *J. Geophys. Res.*, *105*, 15,365–15,377, doi:10.1029/2000JD900185.

Finkelstein, P. L. (2001), Deposition velocities of SO_2 and O_3 over agricultural and forest ecosystems, *Water Air Soil Pollut.: Focus*, *1*, 49–57.

Foken, T. (2006), 50 years of the Monin-Obukhov similarity theory, *Boundary Layer Meteorol.*, doi:10.1107/s10546-006-9048-6.

Foken, T. (2008), *Micrometeorology*, Springer, Berlin.

Fowler, D., C. Flechard, J. N. Cape, R. L. Storeton-West, and M. Coyle (2001), Measurements of ozone deposition to vegetation quantifying the flux, the stomatal and the non-stomatal components, *Water Air Soil Pollut.*, *130*, 63–74, doi:10.1023/A:1012243317471.

Fowler, D., et al. (2009), Atmospheric composition change: Ecosystems–atmosphere interactions, *Atmos. Environ.*, doi:10.1016/j.atmosenv.2009.07.068.

Fu, Y., and A. P. Tai (2015), Impact of climate and land cover changes on tropospheric ozone air quality and public health in East Asia between 1980 and 2010, *Atmos. Chem. Phys.*, *15*, 10,093–10,106, doi:10.5194/acp-15-10093-2015.

Fuentes, J. D., T. J. Gillespie, G. den Hartog, and H. H. Neumann (1992), Ozone deposition onto a deciduous forest during dry and wet conditions, *Agric. For. Meteorol.*, *62*, 1–18.

Fumagalli, I., C. Gruening, R. Marzuoli, S. Cieslik, and G. Gerosa (2016), Long-term measurements of NO_x and O_3 soil fluxes in a temperate deciduous forest, *Agric. For. Meteorol.*, *228*, 205–216, doi:10.1016/j.agrformet/2016.07.011.

Ganzeveld, L., and J. Lelieveld (1995), Dry deposition parameterization in a chemistry general circulation model and its influence on the distribution of reactive trace gases, *J. Geophys. Res.*, *100*, 20,999–21,012.

Ganzeveld, L., L. Bouwman, E. Stehfest, D. P. van Vuuren, B. Eickhout, and J. Lelieveld (2010), Impact of future land use and land cover changes on atmospheric chemistry-climate interactions, *J. Geophys. Res.*, *115*, D23301, doi:10.1029/2010JD014041.

Ganzeveld, L., C. Ammann, and B. Loubet (2015), Modelling atmosphere-biosphere exchange of ozone and nitrogen oxides, in *Review and Integration of Biosphere-Atmosphere Modelling of Reactive Trace Gases and Volatile Aerosols*, edited by: R.-S. Massad and B. Loubet, pp. 85–105, Springer, Netherlands.

Gao, W., and M. L. Wesely (1995), Modeling gaseous dry deposition over regional scales with satellite observations—I. Model development, *Atmos. Environ.*, *29*(6), 727–737, doi:10.1016/1352-2310(94)00284-R.

Gerosa, G., A. Finco, S. Mereu, M. Vitale, F. Manes, and A. B. Denti (2009), Comparison of seasonal variations of ozone exposure and fluxes in a Mediterranean Holm oak forest between the exceptionally dry 2003 and the following year, *Environ. Pollution*, *157*(5), 1737–1744, doi:10.1016/j.envpol.2007.11.025.

Goldstein, A. H., M. McKay, M. R. Kurpius, G. W. Schade, A. Lee, R. Holzinger, and R. A. Rasmussen (2004), Forest thinning experiment confirms ozone deposition to forest canopy is dominated by reaction with biogenic VOCs, *Geophys. Res. Lett.*, *31*, L22106, doi:10.1029/2004GL021259.

Goulden, M. L., J. W. Munger, S. M. Fan, B. C. Daube, and S. C. Wofsy (1996), Measurements of carbon sequestration by long term eddy covariance: Methods and a critical evaluation of accuracy, *Global Change Biol.*, *2*(3), 169–182.

Hardacre, C., O. Wild, and L. Emberson (2015), An evaluation of ozone dry deposition in global scale chemistry climate models, *Atmos. Chem. Phys.*, *15*(11), 6419–6436, doi:10.5194/acp-15-6419-2015.

Hallquist, M., et al. (2009), The formation, properties and impact of secondary organic aerosol: Current and emerging issues, *Atmos. Chem. Phys.*, *9*(14), 5155–5236, doi:10.5194/acp-9-5155-2009.

Hogg, A., J. Uddling, D. Ellsworth, M. A. Carroll, S. Pressley, B. Lamb, and C. Vogel (2007), Stomatal and non stomatal fluxes of ozone to a northern mixed hardwood forest, *Tellus B*, *59*(3), 514–525, doi:10.1111/j.1600-0889.2007.00269.x.

Holmes, C. D. (2014), Air pollution and forest water use, *Nature*, *507*(7491), E1–E2, doi:10.1038/nature13113.

Horii, C. V., J. W. Munger, S. C. Wofsy, M. Zahniser, D. Nelson, and J. B. McManus (2004), Fluxes of nitrogen oxides over a temperate deciduous forest, *J. Geophys. Res.*, *109*, D08305, doi:10.1029/2003JD004326.

Hoshika, Y., G. Katata, M. Deushi, M. Watanabe, T. Koike, and E. Paoletti (2015), Ozone-induced stomatal sluggishness changes carbon and water balance of temperate deciduous forests, *Sci. Rep.*, *5*, doi:10.1038/srep09871.

Högström, U. (1988), Non-dimensional wind and temperature profiles in the atmospheric surface layer: A re-evaluation, *Boundary-Layer Meteorol.*, *42*, 55–78.

Jensen, N. O., and P. Hummelshøj (1995), Derivation of canopy resistance for water vapour fluxes over a spruce forest, using a new technique for the viscous sublayer resistance, *Agric. For. Meteorol.*, *73*, 339–352.

Jensen, N. O., and P. Hummelshøj (1997), Erratum to "Derivation of canopy resistance for water vapour fluxes over a spruce forest, using a new technique for the viscous sublayer resistance", *Agric. For. Meteorol.*, *85*, 289.

Jeong, S.-J., D. Medvigy, E. Shevliakova, and S. Malyshev (2012), Uncertainties in terrestrial carbon budgets related to spring phenology, *J. Geophys. Res.*, *117*, G01030, doi:10.1029/2011JG001868.

Keenan, T. F., D. Y. Hollinger, G. Bohrer, D. Dragoni, J. W. Munger, H. P. Schmid, and A. D. Richardson (2013), Increase in forest water-use efficiency as atmospheric carbon dioxide concentrations rise, *Nature*, *499*(7458), 324–327, doi:10.1038/nature12291.

Keenan, T. F., D. Y. Hollinger, G. Bohrer, D. Dragoni, J. W. Munger, H. P. Schmid, and A. D. Richardson (2014), Keenan et al. reply, *Nature*, *507*(7491), E2–E3, doi:10.1038/nature13114.

Kurpius, M. R., and A. H. Goldstein (2003), Gas-phase chemistry dominates O_3 loss to a forest, implying a source of aerosols and hydroxyl radicals to the atmosphere, *Geophys. Res. Lett.*, *30*(7), 1371, doi:10.1029/2002GL016785.

Lamaud, E., B. Loubet, M. Irgine, P. Stella, E. Personne, and P. Cellier (2009), Partitioning of ozone deposition over a developed maize crop between stomatal and non-stomatal uptakes, using eddy-covariance flux measurements and modelling, *Agric. For. Meteorol.*, *149*, 1385–1396, doi:10.1016/j.agrformet.2009.03.017.

Launiainen, S., G. G. Katul, T. Grönholm, and T. Vesala (2013), Partitioning ozone fluxes between canopy and forest floor by measurements and a multi-layer model, *Agric. For. Meteorol.*, *173*, 85–99, doi:10.1016/j.agrformet.2012.12.009.

Lelieveld, J., and F. J. Dentener (2000), What controls tropospheric ozone?, *J. Geophys. Res.*, *105*, 3531–3551, doi:10.1029/1999JD901011.

Leuning, R. (1995), A critical appraisal of a combined stomatal photosynthesis model for C_3 plants, *Plant Cell Environ.*, *18*(4), 339–355, doi:10.1111/j.1365-3040.1995.tb00370.x.

Lin, Y. S., et al. (2015), Optimal stomatal behaviour around the world, *Nat. Clim. Change*, *5*(5), 459–464, doi:10.1038/nclimate2550.

Lombardozzi, D., J. P. Sparks, and G. Bonan (2013), Integrating O_3 influences on terrestrial processes: Photosynthetic and stomatal response data available for regional and global modeling, *Biogeosciences*, *10*, 6815–6831, doi:10.5194/bg-10-6815-2013.

Lombardozzi, D., S. Levis, G. Bonan, P. G. Hess, and J. P. Sparks (2015), The influence of chronic ozone exposure on global carbon and water cycles, *J. Clim.*, *28*, 292–305, doi:10.1175:JCLI-D-14-00223.1.

Massman, W. J., J. Pederson, A. Delany, D. Grantz, G. Den Hartog, H. H. Neumann, S. P. Oncley, R. Pearson, and R. H. Shaw (1994), An evaluation of the regional acid deposition model surface module for ozone uptake at three sites in the San Joaquin Valley of California, *J. Geophys. Res.*, *99*, 8281–8294, doi:10.1029/93JD03267.

Massman, W. J. (1999), A model study of kB H^{-1} for vegetated surfaces using 'localized near-field' Lagrangian theory, *J. Hydrol.*, *223*(1), 27–43, doi:10.1016/S0022-1694(99)00104-3.

McKinney, K. A., B. H. Lee, A. Vasta, T. V. Pho, and J. W. Munger (2011), Emissions of isoprenoids and oxygenated biogenic volatile organic compounds from a New England mixed forest, *Atmos. Chem. Phys.*, *11*, 4807–4831, doi:10.5194/acp-11-4807-2011.

Medlyn, B. E., R. A. Duursma, D. Eamus, D. S. Ellsworth, I. C. Prentice, C. V. Barton, K. Y. Crous, P. de Angelis, M. Freeman, and L. Wingate (2011), Reconciling the optimal and empirical approaches to modelling stomatal conductance, *Global Change Biol.*, *17*(6), 2134–2144, doi:10.1111/j.1365-2486.2010.02375.x.

Meyers, T. P., P. Finkelstein, J. Clarke, T. G. Ellestad, and P. F. Sims (1998), A multilayer model for inferring dry deposition using standard meteorological measurements, *J. Geophys. Res.*, *103*(D17), 22,645–22,661, doi:10.1029/98JD01564.

Mikkelsen, T. N., H. Ro-Poulsen, K. Pilegaard, M. F. Hovmand, N. O. Jensen, C. S. Christensen, and P. Hummelshoej (2000), Ozone uptake by an evergreen forest canopy: Temporal variation and possible mechanisms, *Environ. Pollut.*, *109*, 423–429.

Mikkelsen, T. N., H. Ro-Poulsen, M. F. Hovmand, N. O. Jensen, K. Pilegaard, and A. H. Egeløv (2004), Five-year measurements of ozone fluxes to a Danish Norway spruce canopy, *Atmos. Environ.*, *38*, 2361–2371, doi:10.1016/j.atmosenv.2003.12.036.

Milly, P. C. D., S. L. Malyshev, E. Shevliakova, K. A. Dunne, K. L. Findell, T. Gleeson, Z. Liang, P. Phillipps, R. J. Stouffer, and S. Swenson (2014), An enhanced model of land water and energy for global hydrologic and earth-system studies, *J. Hydrometeorol.*, 1739–1961, doi:101175/JHM-D-13-0162.1.

Moore, K. E., D. R. Fitzjarrald, R. K. Sakai, M. J. Goulden, J. W. Munger, and S. C. Wofsy (1996), Seasonal variation in radiative and turbulent exchange at a deciduous forest in central Massachusetts, *J. Appl. Meteorol.*, *35*, 122–134.

Munger, J. W., S. C. Wofsy, P. S. Bakwin, S.-M. Fan, M. L. Goulden, B. C. Daube, A. H. Goldstein, K. E. Moore, and D. R. Fitzjarrald (1996), Atmospheric deposition of reactive nitrogen oxides and ozone in a temperate deciduous forest and a subarctic woodland 1. Measurements and mechanisms, *J. Geophys. Res.*, *101*(D7), 12,639–12,657, doi:10.1029/96JD00230.

Munger, J. W., and S. Wofsy (1999a), *Biomass Inventories at Harvard Forest EMS Tower Since 1993, HF069*, Harvard Forest Data Archive, Harvard Forest, Petersham, MA, USA.

Munger, J. W., and S. Wofsy (1999b), *Canopy-Atmosphere Exchange of Carbon, Water and Energy at Harvard Forest EMS Tower Since 1991, HF004*, Harvard Forest Data Archive, Harvard Forest, Petersham, MA, USA.

Neirynck, J., B. Gielen, I. A. Janssens, and R. Ceulemans (2012), Insights into ozone deposition patterns from decade-long ozone flux measurements over a mixed temperate forest, *J. Environ. Monit.*, *14*(6), 1684–1695, doi:10.1039/C2EM10937A.

Nunn, A. J., S. Cieslik, U. Metzger, G. Wieser, and R. Matyssek (2010), Combining sap flow and eddy covariance approaches to derive stomatal and non-stomatal O_3 fluxes in a forest stand, *Environ. Pollut.*, *158*, 2014–2022, doi:10.1016/j.envpol.2009.11.034.

Padro, J. (1996), Summary of ozone dry deposition velocity measurements and model estimates over vineyard, cotton, grass and deciduous forest in summer, *Atmos. Environ.*, *30*(11), 2363–2369.

Park, R. J., S. K. Hong, H.-A. Kwon, S. Kim, A. Guenther, J.-H. Woo, and C. P. Loughner (2014), An evaluation of ozone dry deposition simulations in East Asia, *Atmos. Chem. Phys.*, *14*, 7929–7940, doi:10.5194/acp-14-7929-2014.

Paulson, C. A. (1970), The mathematical representation of wind speed and temperature profiles in the unstable atmospheric surface layer, *J. Appl. Meteorol.*, *9*, 857–861.

Pleim, J., and L. Ran (2011), Surface flux modeling for air quality applications, *Atmosphere*, *2*(3), 271–302, doi:10.3390/atmos2030271.

O'Dowd, C. D., P. Aalto, K. Hmeri, M. Kulmala, and T. Hoffmann (2002), Aerosol formation: Atmospheric particles from organic vapours, *Nature*, *416*(6880), 497–498, doi:10.1038/416497a.

Ran, L., J. Pleim, R. Gilliam, F. S. Binkowski, C. Hogrefe, and L. Band (2016), Improved meteorology from an updated WRF/CMAQ modeling system with MODIS vegetation and albedo, *J. Geophys. Res. Atmos.*, *121*, 2393–2415, doi:10.1002/2015JD024406.

Rannik, Ü., N. Altimir, I. Mammarella, J. Bäck, J. Rinne, T. M. Ruuskanen, P. Hari, T. Vesala, and M. Kulmala (2012), Ozone deposition into a boreal forest over a decade of observations: Evaluating deposition partitioning and driving variables, *Atmos. Chem. Phys.*, *12*, doi:10.5194/acp-12-12165-2012.

Richardson, A. D., et al. (2006), A multi-site analysis of random error in tower-based measurements of carbon and energy fluxes, *Agric. For. Meteorol.*, *136*(1), 1–18.

Rienecker, M. M., et al. (2011), MERRA: NASA's modern-era retrospective analysis for research and applications, *J. Clim.*, *24*(14), 3624–3648.

Savage, K. E., and E. A. Davidson (2001), Interannual variation of soil respiration in two New England forests, *Global Biogeochem. Cycles*, doi:10.1029/1999GB001248.

Schwede, D., L. Zhang, R. Vet, and G. Lear (2011), An intercomparison of the deposition models used in the CASTNET and CAPMoN networks, *Atmos. Environ.*, *45*(6), 1337–1346, doi:10.1016/j.atmosenv.2010.11.050.

Sheffield, J., G. Goteti, and E. F. Wood (2006), Development of a 50-year high-resolution global dataset of meteorological forcings for land surface modeling, *J. Clim.*, *19*(13), 3088–3111, doi:10.1175/JCLI3790.1.

Shevliakova, E., S. W. Pacala, S. Malyshev, G. C. Hurtt, P. C. D. Milly, J. P. Caspersen, L. T. Sentman, J. P. Fisk, C. Wirth, and C. Crevoisier (2009), Carbon cycling under 300 years of land use change: Importance of the secondary vegetation sink, *Global Biogeochem. Cycles*, *23*, doi:10.1029/2007GB003176.

Shuttleworth, W. J., et al. (1984), Eddy correlation measurements of energy partition for Amazonian forest, *Quart. J. Roy. Meteorol. Soc.*, doi:10.1002/qj.49711046622.

Sitch, S., P. M. Cox, W. J. Collins, and C. Huntingford (2007), Indirect radiative forcing of climate change through ozone effects on the land-carbon sink, *Nature*, doi:10.1038/nature06059.

Stevenson, D. S., et al. (2006), Multimodel ensemble simulations of present-day and near-future tropospheric ozone, *J. Geophys. Res.*, doi:10.1029/2005JD006338.

Sun, G., S. B. McLaughlin, J. H. Porter, J. Uddling, P. J. Mulholland, M. B. Adams, and N. Pederson (2012), Interactive influences of ozone and climate on streamflow of forested watersheds, *Global Change Biol.*, *18*, 3395–3409, doi:10.1111/j.1365-2486.2012.02787.x.

Turnipseed, A. A., S. P. Burns, D. J. Moore, J. Hu, A. B. Guenther, and R. K. Monson (2009), Controls over ozone deposition to a high elevation subalpine forest, *Agric. For. Meteorol.*, *149*(9), 1447–1459, doi:10.1016/j.agrformet.2009.04.001.

Urbanski, S., C. Barford, S. Wofsy, C. Kucharik, E. Pyle, J. Budney, K. McKain, D. Fitzjarrald, M. Czikowsky, and J. W. Munger (2007), Factors controlling CO_2 exchange on timescales from hourly to decadal at Harvard Forest, *J. Geophys. Res.*, *112*, *G02020*, doi:10.1029/2006JG000293.

Val Martin, M., C. L. Heald, and S. R. Arnold (2014), Coupling dry deposition to vegetation phenology in the Community Earth System Model: Implications for the simulation of surface O_3, *Geophys. Res. Lett.*, *41*, 2988–2996, doi:10.1002/2014GL059651.
van Donkelaar, A., et al. (2008), Analysis of aircraft and satellite measurements from the Intercontinental Chemical Transport Experiment (INTEX-B) to quantify long-range transport of East Asian sulfur to Canada, *Atmos. Chem. Phys.*, *8*, 2999–3014.
Walker, T. W. (2014), Applications of adjoint modelling in chemical composition: Studies of tropospheric ozone at middle and high northern latitudes, PhD thesis, Univ. of Toronto, Toronto, Canada.
Wang, Y., D. J. Jacob, and J. A. Logan (1998), Global simulation of tropospheric O_3-NO_x-hydrocarbon chemistry, 1. Model formulation, *J. Geophys. Res.*, *103*, 10,713–10,726, doi:10.1029/98JD00158.
Wehr, R., J. W. Munger, J. B. McManus, D. D. Nelson, M. S. Zahniser, E. A. Davidson, S. C. Wofsy, and S. R. Saleska (2016), Seasonality of temperate forest photosynthesis and daytime respiration, *Nature*, *534*, 680–683, doi:10.1038/nature17966.
Wesely, M. L., and B. B. Hicks (1977), Some factors that affect the deposition rates of sulfur dioxide and similar gases on vegetation, *J. Air Pollut. Control Assoc.*, *27*, 1110–1116, doi:10.1080/00022470.1977.10470534.
Wesely, M. L. (1989), Parameterization of surface resistances to gaseous dry deposition in regional-scale numerical models, *Atmos. Environ.*, *23*(6), 1293–1304.
Wesely, M. L., and B. B. Hicks (2000), A review of the current status of knowledge on dry deposition, *Atmos. Environ.*, *34*(12), 2261–2282, doi:10.1016/S1352-2310(99)00467-7.
Wild, O. (2007), Modelling the tropospheric ozone budget: Exploring the variability in current models, *Atmos. Chem. Phys.*, *7*, 2643–2660.
Wittig, V. E., E. A. Ainsworth, S. L. Naidu, D. S. Karnosky, and S. P. Long (2009), Quantifying the impact of current and future tropospheric ozone on tree biomass, growth, physiology and biochemistry: A quantitative meta analysis, *Global Change Biol.*, doi:10.1111/j.1365-2486.2008.01774.x.
Wolfe, G. M., J. A. Thornton, M. McKay, and A. H. Goldstein (2011), Forest-atmosphere exchange of ozone: Sensitivity to very reactive biogenic VOC emissions and implications for in-canopy photochemistry, *Atmos. Chem. Phys.*, *11*(15), 7875–7891, doi:10.5194/acp-11-7875-2011.
Wu, S., L. J. Mickley, J. O. Kaplan, and D. J. Jacob (2012), Impacts of changes in land use and land cover on atmospheric chemistry and air quality over the 21st century, *Atmos. Chem. Phys.*, *12*, 1597–1609, doi:10.5194/acp-12-1597-2012.
Wu, Z., X. Wang, F. Chen, A. Turnipseed, A. Guenther, D. Niyogi, U. Charusombat, B. Xia, W. Munger, and K. Alapaty (2011), Evaluating the calculated dry deposition velocities of reactive nitrogen oxides and ozone from two community models over a temperate deciduous forest, *Atmos. Environ.*, *45*, doi:10.1016/j.atmosenv.2011.02.063.
Wu, Z. Y., L. Zhang, X. M. Wang, and J. W. Munger (2015), A modified micrometeorological gradient method for estimating O_3 dry depositions over a forest canopy, *Atmos. Chem. Phys.*, doi:10.5194/acp-15-7487-2015.
Young, P. J., et al. (2013), Pre-industrial to end 21st century projections of tropospheric ozone from the Atmospheric Chemistry and Climate Model Intercomparison Project (ACCMIP), *Atmos. Chem. Phys.*, doi:10.5194/acp-13-2063-2013.
Yue, X., T. F. Keenan, W. Munger, and N. Unger (2016), Limited effect of ozone reductions on the 20 year photosynthesis trend at Harvard Forest, *Global Change Biol.*, doi:10.1111/gcb.13300.
Zeller, K. F., and N. T. Nikolov (2000), Quantifying simultaneous fluxes of ozone, carbon dioxide and water vapor above a subalpine forest ecosystem, *Environmental Pollution*, *107*, 1–20.
Zhang, L., J. R. Brook, R. Vet, M. Shaw, and P. L. Finkelstein (2001), Evaluation and improvement of a dry deposition model using SO_2 and O_3 measurements over a mixed forest, *Water, Air, Soil Pollut.: Focus*, *1*, 67–78.
Zhang, L., J. R. Brook, and R. Vet (2002), On ozone dry deposition—With emphasis on non-stomatal uptake and wet canopies, *Atmos. Environ.*, *36*, 4787–4799.
Zhang, L., J. R. Brook, and R. Vet (2003), A revised parameterization for gaseous dry deposition in air-quality models, *Atmos. Chem. Phys.*, *3*, 2067–2082.
Zhang, L., R. Vet, J. R. Brook, and A. H. Legge (2006), Factors affecting stomatal uptake of ozone by different canopies and a comparison between dose and exposure, *Sci. Total Environ.*, *370*, 117–132.
Zona, D., B. Gioli, S. Fares, T. De Groote, K. Pilegaard, A. Ibrom, and R. Ceulemans (2014), Environmental controls on ozone fluxes in a poplar plantation in western Europe, *Environ. Pollut.*, *184*, 201–210, doi:10.1016/j.envpol.2013.08.032.

Erratum

In the originally published version of this article, the author incorrectly calculated the average of the wind direction (wdirc) in Table S1 of the supplementary information. It was calculated as an arithmetic mean, and the calculation was changed because wind direction is a circular variable. This version may be considered the version of record.